Cerebral Cortex, 2021;00: 1–15

https://doi.org/10.1093/cercor/bhab304
Original Article

ORIGINAL ARTICLE

Hippocampal Representations of Event Structure and Temporal Context during Episodic Temporal Order Memory

Chuqi Liu[1], Zhifang Ye[1,2], Chuansheng Chen[3], Nikolai Axmacher[1,4] and Gui Xue[1]

[1]State Key Laboratory of Cognitive Neuroscience and Learning & IDG/McGovern Institute of Brain Research, Beijing Normal University, Beijing 100875, PR China, [2]Department of Psychology, University of Oregon, Eugene, OR 97403, USA, [3]Department of Psychological Science, University of California, Irvine, CA 92697, USA and [4]Department of Neuropsychology, Institute of Cognitive Neuroscience, Faculty of Psychology, Ruhr University Bochum, Bochum 44801, Germany

Address correspondence to Gui Xue. Email: gxue@bnu.edu.cn

Abstract

The hippocampus plays an important role in representing spatial locations and sequences and in transforming representations. How these representational structures and operations support memory for the temporal order of random items is still poorly understood. We addressed this question by leveraging the method of loci, a powerful mnemonic strategy for temporal order memory that particularly recruits hippocampus-dependent computations of spatial locations and associations. Applying representational similarity analysis to functional magnetic resonance imaging activation patterns revealed that hippocampal subfields contained representations of multiple features of sequence structure, including spatial locations, location distance, and sequence boundaries, as well as episodic-like temporal context. Critically, the hippocampal CA1 exhibited spatial transformation of representational patterns, showing lower pattern similarity for items in same locations than closely matched different locations during retrieval, whereas the CA23DG exhibited sequential transformation of representational patterns, showing lower pattern similarity for items in near locations than in far locations during encoding. These transformations enabled the encoding of multiple items in the same location and disambiguation of adjacent items. Our results suggest that the hippocampus can flexibly reconfigure multiplexed event structure representations to support accurate temporal order memory.

Key words: event structure, hippocampal subfields, method of loci, temporal context reinstatement, temporal order memory

Introduction

Episodic memory is inherently structured according to the temporal order of experiences (Tulving 1985). As the core brain structure for spatial navigation and episodic memory, the hippocampus and surrounding areas of the medial temporal lobe (MTL) have been consistently implicated in spatial and temporal coding in rodents and humans (Eichenbaum 2014; Davachi and DuBrow 2015; Ranganath and Hsieh 2016). In particular, the hippocampal–entorhinal system supports representations of temporally ordered events via sequential activation of spatially tuned cells (Buzsáki and Llinás 2017), suggesting that space and time can be unified into a common internal coding scheme.

Recent rodent research has revealed 2 types of temporal order representation in the hippocampal–entorhinal system: The representations of stable event sequence increased in well-practiced structured events, and the temporal flow that is formed automatically with one-shot learning (Tsao et al. 2018). Human functional imaging studies have implicated the hippocampus and the anterior-lateral entorhinal cortex (alEC) in the representation of event structure (Deuker et al. 2016; Bellmund et al. 2019), and recall of temporal order of real-life events from a movie (Montchal et al. 2019). Although temporal context binding has been consistently implicated in temporal order judgment (Howard and Kahana 2002; Howard et al. 2005; Ezzyat and Davachi 2014; Jenkins and Ranganath 2016), little is known regarding how the learned event structure can be used as a scaffold to support effective temporal order memory.

This question is critical for the understanding of human temporal order memory, because people are generally bad at one-shot, episodic-like temporal order memory for random events, perhaps because the contextual drifts may be rather nonlinear and unstable. By contrast, learned event structures may be used to dramatically boost performance. In fact, ancient Greek and Roman orators had long realized that linking novel material to sequential locations along a familiar and well-organized route could significantly improve temporal order memory (Roediger 1980). Since then, this mnemonic strategy, called the method of loci or memory palace, has been commonly used by memory experts and athletes (Maguire et al. 2003). Several studies have shown that the method of loci primarily engages spatial and associative processes in the MTL (Maguire et al. 2003; Fellner et al. 2016; Dresler et al. 2017), as well as the interaction between the hippocampus and caudate (Müller et al. 2018).

The current study aimed to examine the hippocampal spatiotemporal representations while subjects were using the method of loci for temporal order memory. First, we would predict that the temporal context and spatial sequence (including spatial location and sequence order) were encoded in the same hippocampal–entorhinal system, which would be late reactivated during retrieval as suggested by a recent rodent study (Tsao et al. 2018). Second, in order to differentiate temporally adjacent items, some representational transformations of temporal information would be necessary. Finally, since in practice each location is usually used for multiple items, precise temporal order memory of multiple items in the same location would require strong temporal context coding and/or transformations of spatial representations. We tested these hypotheses by combining the ancient mnemonic strategy of the method of loci and representational similarity analysis (RSA) of functional magnetic resonance imaging (fMRI) data. Our study revealed multiplexed representations of event structure containing spatial location, sequential order and boundary, and temporal context in the human hippocampus. More critically, the event structure representations in the hippocampus exhibited representational transformations in spatial and sequential patterns, suggesting that the hippocampus may flexibly reconfigure event representations to optimize temporal order memory.

Materials and Methods

Participants

Twenty-nine college students (10 males; ages 18–24 years, mean age = 20.3 years) participated in this experiment. All of them were healthy, had normal or corrected-to-normal vision, and no history of psychiatric of neurological diseases. None of them had experience or practice with the method of loci before the experiment. Two additional subjects were also recruited but removed from final analysis (one did not finish the scan session and one had extremely low memory performance with less than 2% remembered trials). Written consent was obtained from each participant after a full explanation of the study procedure. The study was approved by the Institutional Review Boards at Beijing Normal University and the Center for MRI Research at Peking University.

Experimental Stimuli

The stimuli consisted of 270 two-character Chinese words that were randomly divided into 9 lists of 30 words each. Sixty words were used in the baseline test (2 lists), 150 in practice sessions (5 lists), and 60 in the scanning session (2 lists). All words describe common objects (e.g., broom), animals (e.g., crow), fruits (e.g., lemon), or vegetables (e.g., onion). The same word lists were used in each session and the orders of the words were randomized across subjects.

Experimental Procedure

Subjects completed 5 experimental sessions across 5 consecutive days (Fig. 1A). On day 1, they finished 2 rounds of the temporal order task without using the method of loci, which served as the baseline. Immediately after the task, they were trained with the method of loci mnemonic by watching a 2-h video developed by our lab (see below). On day 2, they were asked to review the method and apply it in the subsequent temporal order task. Only one round of the temporal order memory task was administered (Practice 1). On days 3 and 4, they finished 2 rounds of the temporal order task each day (i.e., Practice 2 and Practice 3) to further improve their method of loci skills. On day 5, they also completed 2 rounds of the temporal order task in the fMRI scanner.

Method of Loci

The method of loci uses visualizations of familiar spatial information to scaffold the memorization of a sequence of other information like words or objects. In short, it is carried out by mentally placing each to-be-remembered item into one specific familiar location, creating vivid mental associations between physical locations and the items. In the present experiment, the same route (i.e., a world map with 10 locations) was introduced for all subjects to let them follow an identical memory route (Fig. 1B). During the 2-h video practice session, they were asked to remember the order of the route and use one landmark for each location to learn to vividly associate the to-be-remembered words with the locations, for example, “the Statue of Liberty in U.S.-apple.” They were free to play back the videos and ask questions about the strategies. We also asked the subjects to explain the method in their own words to make sure they correctly understood. Then they finished several word–location associations and retrieved the words by imagining that they walked through the route. Before each practice session and the scanning session, subjects were asked to rehearse the main points of the method and wrote down the names of the 10 locations in the correct order. We emphasized that they should use the landmarks we provided in the later memory task. All

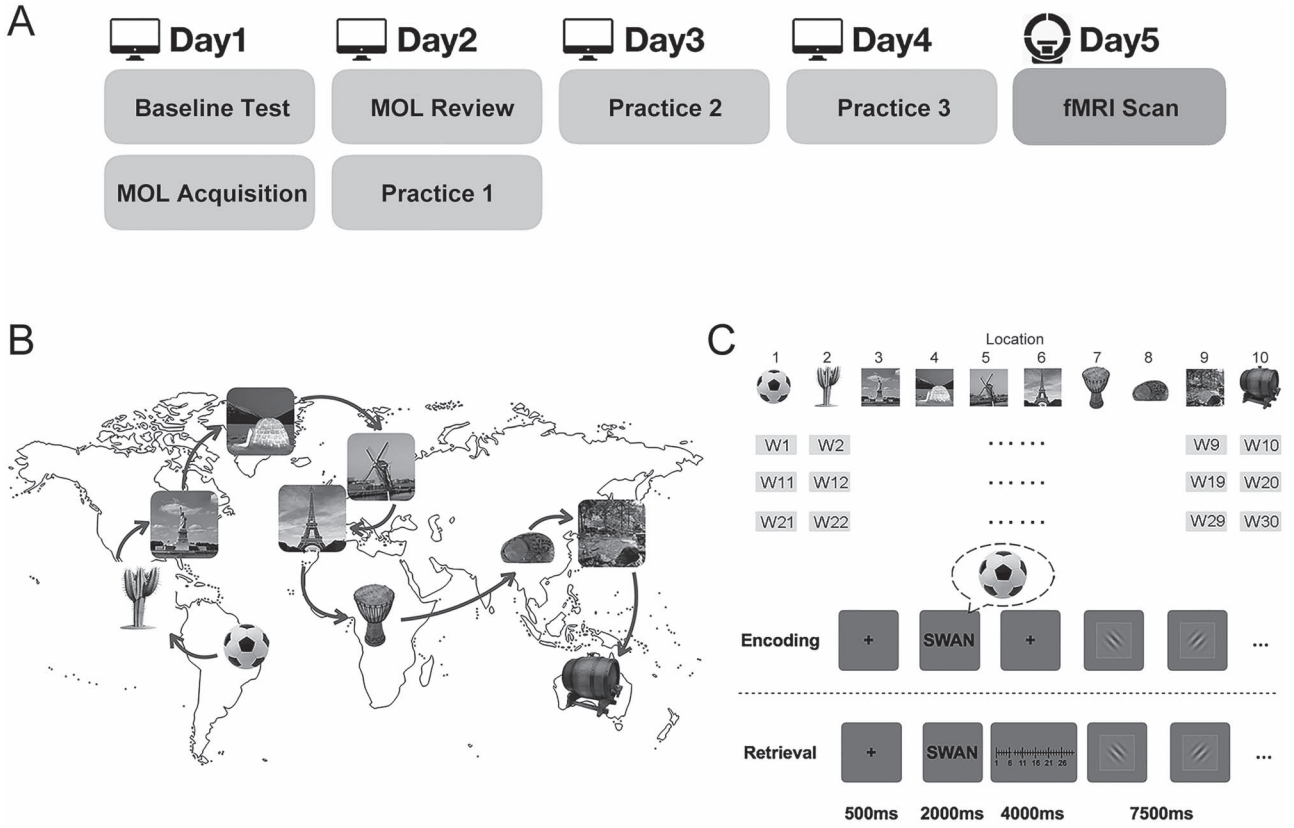

Figure 1. The method of loci and experimental design. (*A*) Subjects completed 5 sessions on 5 consecutive days. On day 1, they conducted a baseline test (2 rounds of the temporal order memory task) and studied the method of loci video for 2 h. On day 2, they reviewed the method of loci method and practiced one round of the temporal order memory task. On days 3 and 4 and during the fMRI scanning, they finished 2 rounds of the temporal order memory task. (*B*) Subjects were trained to remember a sequence of locations and then asked to make associations between these locations and the to-be-learnt words. The same route and landmarks were used for all subjects, with half landmarks were local symbolic entities (objects) and half were famous scenes. (*C*) During encoding, subjects studied a list of 30 words (W1–W30) by mentally associating them with 10 well-trained locations in a fixed order (e.g., the 1st, 11th, and 21st word were associated with location 1). Please note that the loci map was not presented to the subjects. Each word was presented for 2 s, followed by a 4 s fixation cross. Subjects had 6 s to encode the word. During retrieval, a studied word was presented for 2 s and subjects were asked to recall the temporal order in the list. They were then asked to indicate its exact temporal position by moving the red slider on the timeline with the "left" or "right" button in 4 s. Subjects could press the "don't know" button if they could not remember the word or its list position. A slow event-related design (14 s/trial) was used for the encoding and retrieval phases. To prevent subjects from further processing the word, subjects performed a 7.5-s perceptual orientation judgment task after encoding or retrieval each word. The encoding–retrieval cycle was conducted twice in the scanner with 30 different words in each cycle.

subjects performed 3 practice sessions and reported they could properly use the strategy before scanning.

Temporal Order Task

Each temporal order task consisted of an encoding task and a retrieval task (Fig. 1C). The same slow event-related design (14 s for each trial) was used for the baseline test, the practice sessions, and the scanning session and for both encoding and retrieval tasks. During encoding, a fixation cross was presented for 500 ms, followed by the 2-character Chinese word for 2 s. Another fixation was presented for 4 s during which subjects associated the word with the correct location along the path. After that, they performed a perceptual judgment task for 7.5 s. A Gabor image tilting 45° to the left or the right was presented on the screen, and subjects were asked to identify the orientation of the Gabor by pressing 1 of 2 buttons as quickly and accurately as possible. The next Gabor started 100 ms after subjects responded. In each encoding run, subjects learned 30 words in 7 min. The 30 words were associated with 10 locations in a fixed order, and thus, each location was associated with 3 words (e.g., the 1st, 11th, and 21st word in location 1).

Subjects performed a 6-min working memory task between encoding and retrieval. During the baseline test and fMRI scan, a spatial working memory task was used. Each trial started with a 2-s encoding phase, during which 3–6 dots were sequentially displayed for 250 ms on different positions of an (invisible) 5×5 checker board. After an 8-s delay, a probe was presented and subjects were asked to judge whether a dot had been presented in this location during encoding or not. A different working memory task (comprising a 1-back task of one-digit numbers) was used in the 3 practice sessions so that subjects would not be overtrained on the spatial working memory task (which might confound the comparison of behavioral performance between baseline and fMRI scan).

During retrieval, each trial started with a fixation cross shown for 500 ms, followed by a presentation of one of the studied words for 2 s. A scaled timeline was then presented on the screen for 4 s, and subjects were asked to indicate the exact temporal position of the word in the list (i.e., 1–30), by moving

the red slider on the timeline with the "left" or "right" button. The slider would keep moving as long as the subjects held the button down. The initial position of the red slider was randomly selected but was never the correct position for that word. The scale and slider would stay on screen for the whole 4-s period, and the last position of the slider was taken as the response. Subjects could press a "don't know" button if they could not remember the word or its temporal order. Lack of responses was also categorized as "don't know." After the temporal order judgment, subjects performed the same perceptual judgment task as in the encoding task for 7.5 s. Each retrieval run also lasted 7 min. On days 1, 3, 4, and 5 (i.e., during fMRI scan), subjects performed 2 rounds of encoding and retrieval tasks with different sets of 30 words, which were also separated by a working memory task. On day 2, they performed one round. The whole temporal order task lasted 46 min on days 1, 3, 4, and 5 and 20 min on day 2.

MRI Acquisition

Imaging data were acquired on a 3.0T Siemens Prisma MRI scanner with a 64-channel head–neck coil at the MRI Center at Peking University. High-resolution functional images were acquired using a simultaneous multi-slice EPI sequence (time repetition [TR]/time echo [TE]/$\theta = 2000$ ms/30 ms/90°; field of view [FOV] = 198 mm × 198 mm; matrix = 124 × 124; in-plane resolution = 1.6 × 1.6 mm; slice thickness = 1.6 mm; GRAPPA factor = 2; multi-band acceleration factor = 3). Ninety contiguous axial slices parallel to the AC–PC line were obtained to cover the whole cerebrum and partial cerebellum. A high-resolution structural image was acquired for the whole brain using a 3D, T1-weighted MPRAGE sequence (TR/TE/$\theta = 2530$ ms/2.98 ms/7°; FOV = 256 mm × 256 mm; matrix = 256 × 256; slice thickness = 1 mm; GRAPPA factor = 2). A high-resolution T2-weighted image was also acquired using a T2-SPACE sequence for hippocampus segmentation. The image plane was perpendicular to the long axis of the hippocampus and covered the whole MTL region (TR/TE/$\theta = 13\,150$ ms/82 ms/150°; FOV = 220 mm × 220 mm; matrix = 512 × 512; slice thickness = 1.5 mm; 60 slices). A field map was acquired for correction of magnetic field distortions using a Gradient Echo sequence (TR = 767 ms; $\theta = 60°$; TE1/TE2 = 4.92 ms/7.38 ms; FOV = 198 mm × 198 mm; matrix = 124 × 124; slice thickness = 2 mm; 77 slices).

Data Analysis

Image Preprocessing

MRI data were first converted to Brain Imaging Data Structure format (Gorgolewski et al. 2016). The first 10 volumes before the task were automatically discarded by the scanner to allow for T1 stabilization. Image preprocessing was performed using FMRIPrep v1.4.0 (Esteban et al. 2019). Each T1 volume was corrected for intensity using N4BiasFieldCorrection (Tustison et al. 2010) and skull-stripped using antsBrainExtraction.sh (OASIS template). Cortical surfaces were reconstructed using FreeSurfer v6.0.1 (Dale et al. 1999). The T1 volume was then normalized to the ICBM 152 Nonlinear Asymmetrical template (version 2009c) through nonlinear registration with the ANTs v2.1.0 (Avants et al. 2008). Functional data were slice time corrected using AFNI v16.2.07 (Cox 1996), motion-corrected using FSL's MCFLIRT (Jenkinson et al. 2002), and registered to the T1 image using a boundary-based registration with 9 degrees of freedom (Greve and Fischl 2009). For univariate analysis, data were spatially smoothed with a 6-mm full-width-at-half-maximum Gaussian kernel using FSL's SUSAN, filtered in the temporal domain using a nonlinear high-pass filter with a 100 s cutoff, and normalized to Montreal Neurological Institute (MNI) Template space. The univariate analysis involving the hippocampal subfields (region of interest [ROI] analysis) and the RSA analysis were conducted in subjects' native space. For both analyses, slight spatial smoothing was applied to the data using a 1.6-mm full-width-at-half-maximum Gaussian kernel and filtered in the temporal domain using a nonlinear high-pass filter with a 100 s cutoff in order to obtain both high signal-to-noise ratio and anatomical specificity.

Hippocampal Subfields Segmentation

The hippocampus and surrounding MTL areas were segmented into CA1, CA2, CA3, DG, EC, and parahippocampal cortex (PHC) using the automatic segmentation of hippocampal subfields (ASHS) toolbox with the UPenn atlas (Yushkevich et al. 2015). Anatomical masks segmented by ASHS were coregistered to the functional image for further analyses. CA2, CA3, and DG were combined (i.e., CA23DG) because they could not be unambiguously distinguished. This method has been successfully used in previous studies with similar scanning parameters (e.g., Hindy et al. 2016; Sone et al. 2016; Xiao et al. 2017; Bender et al. 2018; Cong et al. 2018; Dimsdale-Zucker et al. 2018; Kok and Turk-Browne 2018). The ASHS algorithms showed reliable subfield segmentation among the studies. To further examine the functional specificity of EC subregions, we segmented the EC into alEC and posterior-medial EC (pmEC), using the masks from a previous publication (Maass et al. 2015). These masks were resampled and aligned into subjects' native space, using nonlinear registration tool ANTs (v2.1.0). They were then intersected with the EC masks generated by ASHS to improve segmentation precision. As a result, our ROIs included CA1, CA23DG, alEC, pmEC, and PHC (1.6 mm^3 resolution, numbers of voxels: CA1 = 683.93 ± 74.31; CA23DG = 440.76 ± 55.52; alEC = 93.45 ± 17.99; pmEC = 63.90 ± 13.00; PHC = 514.59 ± 83.70). Two experimenters visually verified the accuracy of the segmentation.

Univariate Analysis

Models were constructed using the general linear model within the FILM (version 6.00) module of FSL. For both the encoding and retrieval tasks, 2 types of trials were modeled: remembered and forgotten trials. We excluded trials with a temporal error of 1 position, as it was unclear whether these errors were due to inaccurate memory or response errors. The "unsure" trials and orientation trials from both encoding and retrieval were modeled as regressors of no interest. Stimuli were modeled at the onset of presentation with a duration of 2 s. The above regressors were convolved with a double gamma hemodynamic response function. Six movement parameters and the frame-wise displacement (FD) were modeled as confound regressors. Additional censor regressors were included for each volume with a FD greater than 0.3 mm. Each run was modeled separately in the first-level analysis. Cross-run averages for each contrast image were created for each subject using a fixed-effects model. These contrast images were then used for group analyses with a random-effects model. Group images were thresholded using cluster detection statistics, with a height threshold of $z > 2.3$ and a cluster probability of $P < 0.05$, corrected for whole-brain multiple comparisons using Gaussian Random Field Theory.

Region of Interest Analysis

We conducted the percent signal change analysis within the predefined ROIs in the subject's native space. Parameter estimates (β values) of remembered and forgotten trials from the GLM were each averaged across all voxels in a given ROI for each subject. Percent signal changes were calculated using the following formula: (β/mean) × ppheight × 100%, where ppheight is the peak height of the hemodynamic response versus the baseline level of activity (Mumford 2007).

Single-Trial Response Estimations

Single-trial response estimations were done using the least-square separate method for each functional run (Mumford et al. 2012). Each trial was estimated in a separate GLM, in which the given trial was modeled as a separate regressor, whereas all the remaining trials were modeled as another regressor. Again, stimuli were modeled at the onset of presentation with a duration of 2 s, and each regressor was convolved with a double gamma hemodynamic response function. The 6 movement parameters and FD were included in each GLM as confound regressors. Additional censor regressors were included for each volume with a FD greater than 0.3 mm. This resulted in a single β image for each trial, which was used for the representational similarity analysis.

Representational Similarity Analysis

RSA (Kriegeskorte et al. 2008) was used to determine the neural pattern similarity between trial pairs from different conditions. The neural pattern similarities could be calculated between encoding–encoding, retrieval–retrieval, or encoding–retrieval tasks, using images from the same or different runs. The main analysis focused on examining similarities within predefined ROIs (CA1, CA23DG, alEC, pmEC, and PHC). Each trial's β values from the single-trial response estimations within the ROI were extracted. The Fisher *Z*-transformed Pearson's correlations across trials were used as the index of neural pattern similarity. These similarities were then grouped and averaged based on the spatial location, sequence distance, and temporal distance for further statistical analysis. We used all trials for the encoding task but only included remembered trials for the retrieval task to make sure the correct context representations were reinstated. To test group-level significance, paired *t*-tests or repeated measures analyses of variance (ANOVAs) were used and reported (see Statistical Analysis). We also conducted nonparametric permutation tests for group-level significance and the results remained significant.

Whole-Brain Searchlight Analysis

In order to examine the effect beyond our predefined ROIs, a whole-brain searchlight analysis was conducted (Kriegeskorte et al. 2006). Each searchlight was defined as a spherical cluster in the subject's native space with a radius of 3 voxels (4.8 mm, 123 voxels in total) surrounding a target voxel. The neural pattern similarity difference of interest was calculated within the sphere and assigned to the center voxel. All contrast maps of all subjects were transformed into MNI space and entered into group analysis using nonparametric permutation for inference on the statistical map. Nonparametric permutations were conducted by Randomise in FSL with 5000 permutations. The significance of the derived statistical map was determined by the threshold-free cluster enhancement algorithm with $P < 0.05$ (whole-brain FWE corrected) (Smith and Nichols 2009).

Statistical Analysis

All paired *t*-tests and repeated measures ANOVAs in our analysis were 2-tailed and conducted by the afex package using type III sums of squares and using Greenhouse–Geisser correction to correct the degrees of freedom if necessary in R 3.6.1. Error bars in figures denote within-subject standard errors. They were calculated using the Cousineau–Morey–O'Brien method (Cousineau and O'Brien 2014). FDR correction was performed to correct for multiple comparisons across the multiple ROIs.

Results

Behavioral Results

Behavioral analyses showed that across the practice sessions, temporal order memory performance improved dramatically across days ($F(3.43, 95.97) = 60.04$, $P < 0.0001$, $\eta^2 = 0.50$) (Supplementary Fig. 1A), consistent with previous observations that the method of loci can quickly improve temporal order memory (Dresler et al. 2017; Wagner et al. 2021). During the fMRI scanning, the overall accuracy was 49.9% (Fig. 2A). Post hoc *t*-tests (Tukey HSD) revealed that although the accuracy during scanning was slightly lower than during the last practice session (61.9%, $t(28) = -4.04$, $P = 0.003$, Cohen's $d = 0.75$), probably due to the restricted learning environment and noise in the scanner, it was significantly higher than during baseline (19.5%, $t(28) = 8.41$, $P < 0.001$, Cohen's $d = 1.56$) and the first practice session (28.5%, $t(28) = 6.12$, $P < 0.001$, Cohen's $d = 1.14$). It should be noted that although we could not conclusively state that the method of loci improved temporal order memory due to the lack of a strict control condition, the high behavioral precision enabled us to examine the hippocampal representations that support precise temporal order memory.

We further examined the behavioral pattern to ensure that subjects were actually using the method of loci. First, if they were relying on the locations to encode the temporal order of the studied items, we would predict recency and primacy effects based on the 10 locations. In contrast, if subjects were encoding the items serially without the method of loci, we would predict that the recency and primacy effects would be based on the overall list of 30 items. Second, if the subjects used the method of loci and 3 words were encoded for each location, we would expect their accuracy to decrease from the first set of 10 words to the second and third sets because of an increasing load at each location (i.e., the fan effect) (Anderson 1974). Finally, we would also expect significant within-location swap errors (i.e., confusion of items that were 10 or 20 positions apart). The fan effect and within-location swap errors should not occur if subjects did not use the method of loci.

To test these hypotheses, we conducted ANOVAs on the behavioral performance during the fMRI scanning as a function of run (subjects finished 2 runs of 30 words), set of words (1–3), and serial position (initial: locations 1–4; middle: locations 5–7; final: locations 8–10). Since we did not find a significant main effect of run ($F(1, 28) = 2.14$, $P = 0.155$) or interactions with run ($Fs < 3.12$, $Ps > 0.05$), the 2 runs were combined for the following analyses (Fig. 2B). Consistent with our hypotheses, a 2-way ANOVA revealed significant main effects of set ($F(1.99, 55.61) = 24.82$, $P < 0.0001$, $\eta^2 = 0.14$) (Fig. 2C) and serial position ($F(1.91, 53.43) = 7.84$, $P = 0.001$, $\eta^2 = 0.05$) (Fig. 2D), but importantly, no set by serial position interaction ($F(3.23, 90.42) = 0.30$, $P = 0.842$). Planned post hoc *t*-tests indicated that memory performance decreased from set 1 to set 3 ($ts > 2.74$,

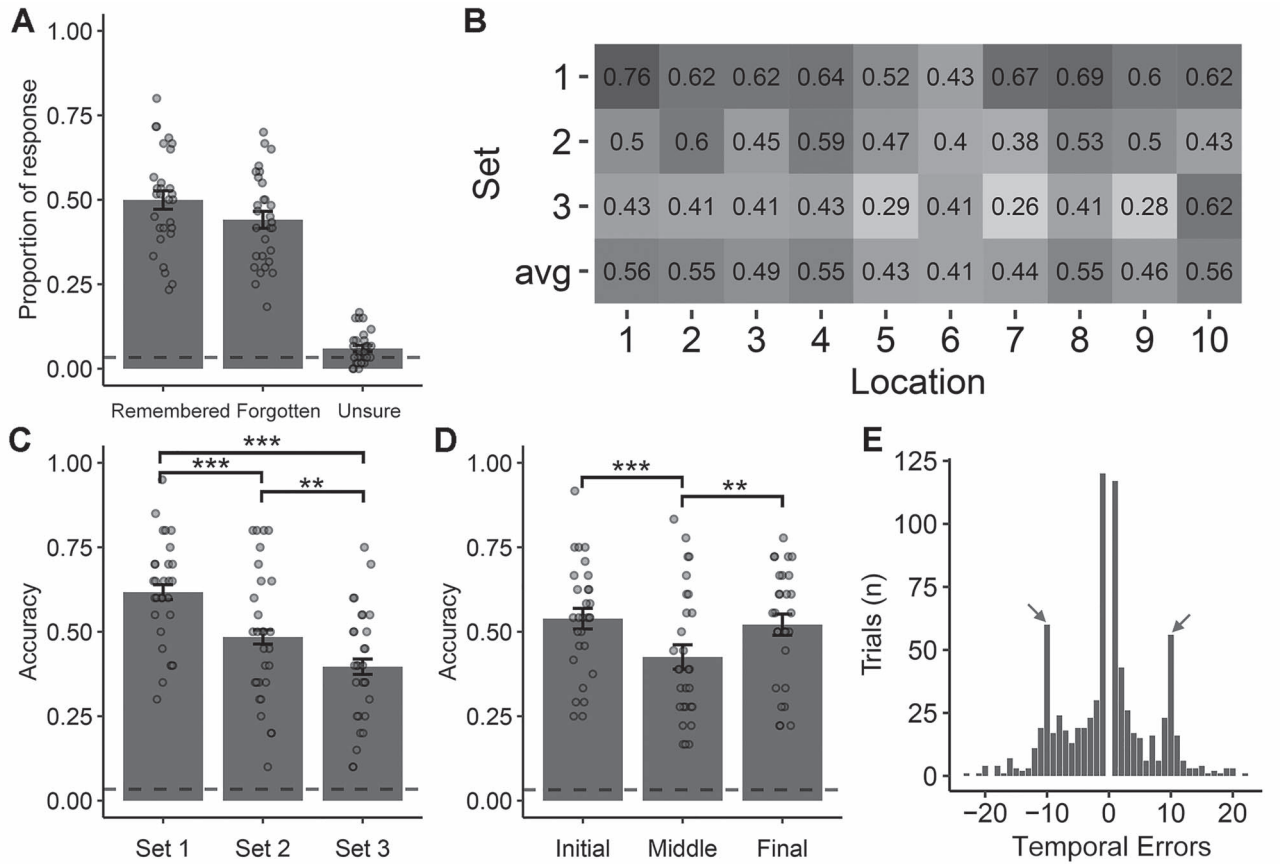

Figure 2. Behavioral results during the fMRI scan. (*A*) Proportions of remembered, forgotten, and unsure trials during fMRI scanning. The dashed line shows the chance level (3.33%). (*B*) Mean accuracy for each location. (*C*) Mean accuracy for each set. There was a significant fan or load effect, that is, memory performance decreased when more items were associated with the same location. The dashed line shows the chance level (3.33%). (*D*) Mean accuracy for different serial positions of the locations (initial: locations 1–4; middle: locations 5–7; final: locations 8–10). There were significant recency and primacy effects across the 10 locations. The dashed line shows the chance level (3.33%). Each dot represents one subject and the bars represent group means. Error bars indicate averaged within-subject standard errors. $^{**}P < 0.01$. $^{***}P < 0.001$. (*E*) The pattern of response errors. Most errors occurred between adjacent locations, followed by within-location swap errors, as indicated by the arrows.

Ps < 0.05, Cohen's *ds* > 0.53), showing a clear fan effect (Fig. 2C). In addition, there were significant recency (final vs. middle, $t(28) = 2.82$, $P = 0.004$, Cohen's $d = 0.52$) and primacy effects (initial vs. middle, $t(28) = 3.81$, $P < 0.001$, Cohen's $d = 0.71$) (Fig. 2D). By examining the pattern of errors, we found that subjects were most likely to confuse items between adjacent locations (237 trials, 13.62% of total trials), followed by within-location swap errors (123 trials, 7.07% of total trials) (Fig. 2E). These results strongly suggest that subjects indeed relied on the 10 locations to encode the words.

A different pattern of results was found for the behavioral data during the baseline test. Specifically, we found a significant set by serial position interaction ($F(3.27, 91.47) = 11.11$, $P < 0.0001$, $\eta^2 = 0.11$), indicating only a primacy effect in set 1 (initial vs. middle/final, *ts* > 5.21, *Ps* < 0.001), but not in sets 2 and 3 (*ts* < 1.78, *Ps* > 0.05) (Supplementary Fig. 2C). No significant within-location swap error was found (Supplementary Fig. 2D). These results suggest that before practice the 30 words were encoded into a single list, rather than based on the 10 locations. Across the baseline and 3 training sessions, the location-based pattern gradually emerged (Supplementary Figs 2–5), showing increased ratios of within-location swap errors to overall errors (Supplementary Fig. 1B). Together, our behavioral data suggest that subjects effectively learned to use the method of loci to encode the word order, which not only improved the overall performance but also changed the behavioral patterns.

fMRI Results

Hippocampal Contributions to Temporal Order Memory

The above behavioral evidence suggests that subjects indeed used the method of loci strategy to aid memory encoding. We then turned to the fMRI data to examine how the employment of this strategy affects activity levels and stimulus-specific representations in hippocampal subfields. The hippocampus and surrounding MTL areas were segmented into 5 regions, including CA1, CA23DG, alEC, pmEC, and PHC (Fig. 3A). The ROI analysis in subjects' native space revealed marginally significant subsequent memory effects (SME) in CA23DG ($t(28) = 2.35$, $P = 0.026$, corrected $P = 0.074$, Cohen's $d = 0.44$) and PHC ($t(28) = 2.29$, $P = 0.030$, corrected $P = 0.074$, Cohen's $d = 0.43$), with subsequently remembered items showing greater activity than subsequently forgotten items (Fig. 3B). Whole-brain univariate analysis in standardized MNI space revealed a significant SME in the left parahippocampal gyrus, the left frontal medial cortex, and the left orbital frontal cortex (FWE-corrected for multiple comparisons), consistent

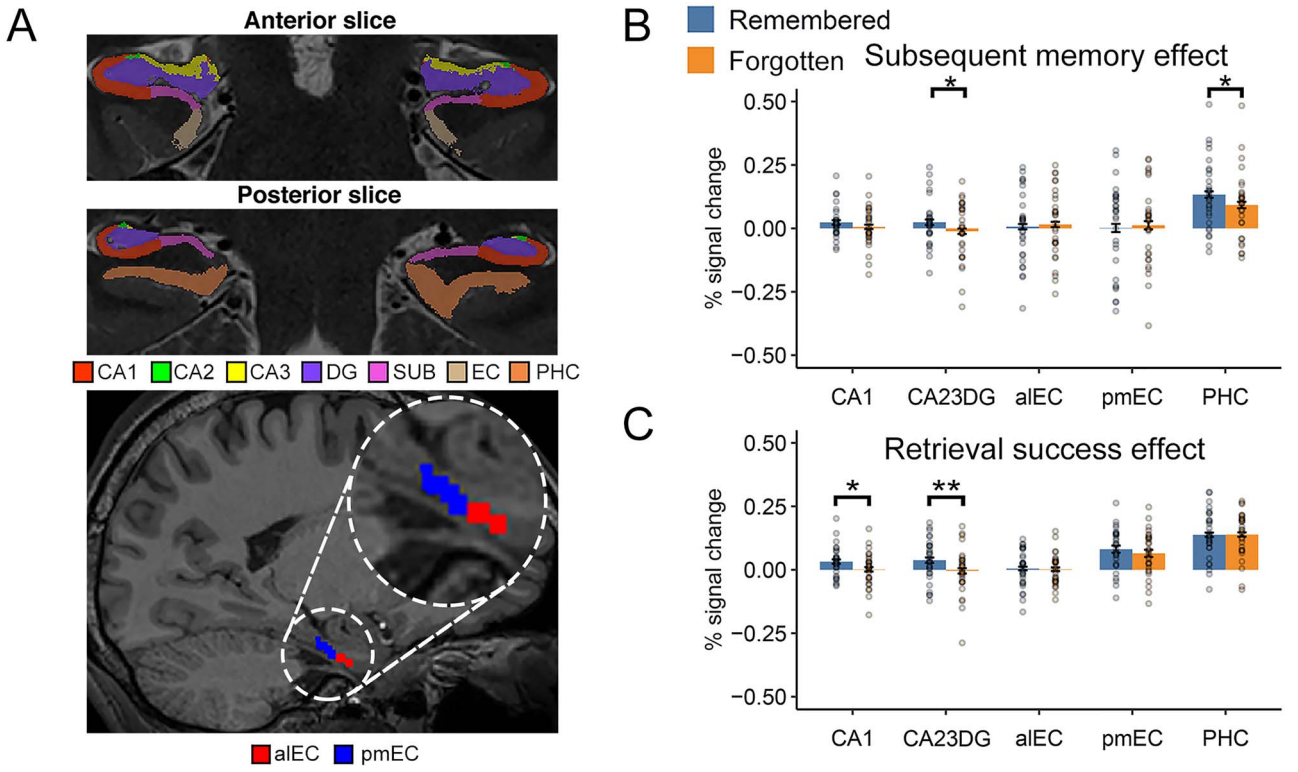

Figure 3. ROIs segmentation and univariate effects of temporal memory. (*A*) Segmentation of hippocampus and adjacent MTL areas. The top 2 panels show an example of segmentation from one subject, which was overlaid onto the subject's T2 image (coronal plane). The hippocampus and surrounding MTL areas were segmented into CA1, CA2, CA3, DG, EC, and PHC using ASHS (Yushkevich et al. 2015). CA2, CA3, and DG were combined because they could not be unambiguously distinguished. The bottom panel shows an example of an EC segment, which was overlaid onto the subject's T1 image (sagittal plane). The EC was segmented into alEC and pmEC, based on published masks (Maass et al. 2015). The masks were resampled and coregistered to each subject's native space and were further intersected with the EC mask generated by ASHS to improve precision. (*B*) SME (remembered > forgotten). (*C*) Retrieval success effects (remembered > forgotten). Each dot represents one subject and the bars represent group means. Error bars indicate averaged within-subject standard errors. $^{*}P < 0.05$ uncorrected. $^{**}P < 0.01$ uncorrected.

with previous observations (Jenkins and Ranganath 2010; Supplementary Fig. 6A; Supplementary Table 1).

During retrieval, we found that the CA1 ($t(28) = 2.50$, $P = 0.018$, corrected $P = 0.046$, Cohen's $d = 0.46$) and CA23DG ($t(28) = 2.84$, $P = 0.008$, corrected $P = 0.042$, Cohen's $d = 0.53$) were more active during remembered than forgotten items (Fig. 3C). Whole-brain univariate analysis revealed several additional brain regions for this contrast, including the bilateral supramarginal gyrus (SMG), bilateral superior parietal lobule (SPL), bilateral lateral occipital cortex (LOC), and bilateral frontal pole (FP) (Supplementary Fig. 6B; Supplementary Table 2). No significant activation was found in the caudate during either encoding or retrieval.

Previous research has revealed stronger hippocampus and PHC activities for scenes than for objects (Zeidman and Maguire 2016). Accordingly, we also conducted a 2 (landmark type: object/scene) × 2 (memory condition: remembered/forgotten) ANOVA in the ROI analysis. This analysis revealed significant main effects of landmark type, but no memory by landmark type interactions ($Ps > 0.135$) (Supplementary Fig. 7).

Hippocampal Representations of Structured Event Sequences

Having shown the involvement of the hippocampus in temporal order memory, we further examined the specific hippocampal representations that supported temporal order memory. In the method of loci strategy, the routes and landmarks were not presented to the subjects during either encoding or retrieval. However, the well-learned mental route could be reactivated and linked with the to-be-learnt words during encoding and again reinstated during retrieval. Both the representations of spatial location and their sequential order/distance are referred as the representations of event structure, which are acquired via the repeated practice of the method of loci mnemonics (Bellmund et al. 2019).

In the first analysis, we examined how the neural pattern similarity was modulated by the distance between 2 locations in the well-trained sequence (Deuker et al. 2016; Bellmund et al. 2019). Note that distance here refers to the ordinal distance between 2 locations (ranging from 1 to 9) rather than their Euclidean or geodesic distance in the real world. We compared the pattern similarity of words that were encoded at near distance (i.e., ordinal distance = 1), middle distance (i.e., $2 \leq$ ordinal distance ≤ 3), and far distance (i.e., ordinal distance > 3) (Fig. 4A). Since the locations are different for all pairs, this contrast between near versus middle versus far pairs revealed the representation of sequential distance rather than location identity. This analysis was done across runs, so the pattern similarity should not be affected by intrinsic autocorrelations of the blood oxygen level-dependent (BOLD) signal or by the differences in the temporal context. Based on previous studies (Deuker et al. 2016; Bellmund et al. 2019), we would predict greater pattern similarity for near-distance pairs than far-distance pairs. Alternatively, the near-distance pairs might

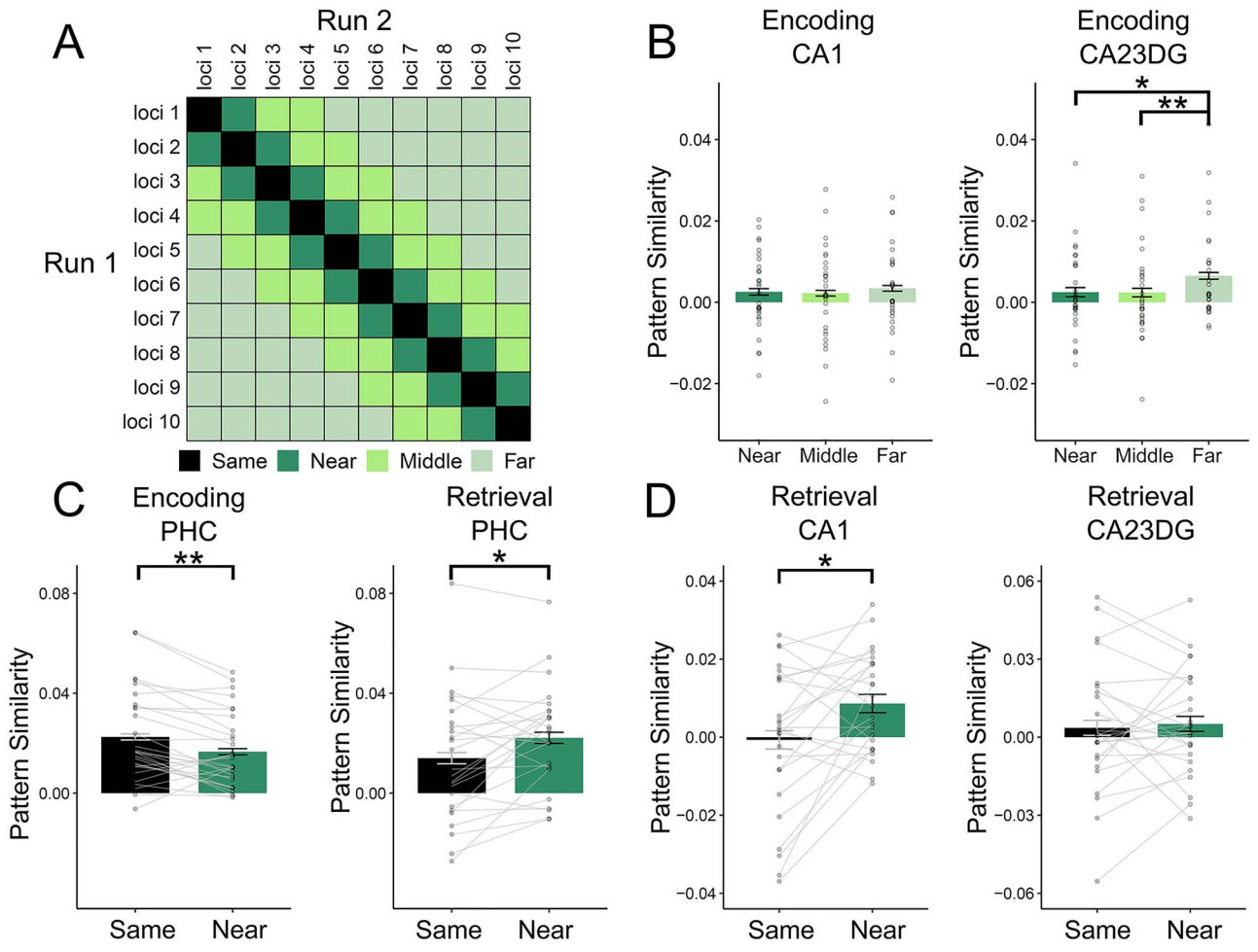

Figure 4. Hippocampal representations of structured location sequences during encoding and retrieval. (*A*) Schematic depiction of word pairs depending on the distance of the associated method of loci locations. Words in a pair are always from different runs. Same: same-location pairs; Near: near-distance pairs (ordinal distance = 1); Middle: middle-distance pairs (2 ≤ ordinal distance ≤ 3); Far: far-distance pairs (ordinal distance > 3). (*B*) Sequence order representations in CA23DG, but not CA1. The CA23DG region showed higher pattern similarity for far-distance pairs than near- and middle-distance pairs. (*C*) Spatial location representations in PHC: higher similarity for same-location than near-distance pairs during encoding, but reversed pattern during retrieval. (*D*) Spatial location representations in CA1, but not CA23DG. Each line represents one subject and the bars represent the group means. Each dot represents one subject and the bars represent the group means. Error bars indicate averaged within-subject standard errors. $^{*}P < 0.05$; $^{**}P < 0.01$.

show lower pattern similarity, so subjects could differentiate the temporal order of adjacent items.

We found that the CA23DG region showed a main effect of location distance during encoding ($F(1.80,50.49) = 5.40$, $P = 0.009$, corrected $P = 0.047$, $\eta^2 = 0.03$). Post hoc *t*-tests (Tukey HSD) showed lower pattern similarity for near-distance pairs than for far-distance pairs ($t(28) = -2.93$, $P = 0.018$, Cohen's $d = 0.54$) and lower pattern similarity for middle-distance pairs than for far-distance pairs ($t(28) = -3.30$, $P = 0.007$, Cohen's $d = 0.61$), but no difference between near- and middle-distance pairs ($t(28) = 0.07$, $P = 0.998$) (Fig. 4*B*). No significant location distance effect was found in CA1 ($F(1.91, 53.39) = 0.668$, $P = 0.510$) or in other MTL subfields (Ps > 0.39). The region (CA1 vs. CA23DG) by location distance interaction was marginally significant ($F(1.64, 45.87) = 3.20$, $P = 0.060$). Note that this result is not critically dependent on how the near-, middle-, and far-distance were defined, as similar results were found with different criteria (Supplementary Fig. 8). A reverse pattern was found in neocortical regions during encoding, with greater neural pattern similarity for near-distance pairs than far-distance pairs in the right occipital pole (OP), bilateral LOC, left SMG/MTG, and left FP (Supplementary Fig. 9; Supplementary Table 3). No significant effect of location distance was found during retrieval.

In a second analysis, we were to examine whether the representation of spatial locations could be identified in the hippocampal subfields. However, since the spatial locations in the present study inherently carried temporal information, a comparison on the pattern similarity of items in the same location with that in different locations was inevitably affected by their differences in the sequential distance (the sequential distance for same-location pairs is 0). To minimize the influence of sequential distance, we compared the pattern similarity of items sharing the same location across 2 runs (i.e., same-location pairs) with those encoding adjacent but different locations (i.e., near-distance pairs, ordinal distance = 1; Fig. 4*A*). This analysis could be performed during both encoding and retrieval (according to the temporal distance during encoding). Again, this cross-run pattern similarity should not be affected by intrinsic autocorrelations of the BOLD signal or by the differences in the temporal context. Based on previous studies on hippocampal

spatial representation (Chanales et al. 2017; Thavabalasingam et al. 2018), we could predict greater pattern similarity for same-location pairs than near-distance pairs. Alternatively, since 3 words were encoded in each locus, the hippocampus might show lower pattern similarity for same-location pairs than near-distance pairs, so subjects could avoid within-location swap errors (Favila et al. 2016).

We found that the PHC showed greater pattern similarity for same-location pairs than near-distance pairs during encoding ($t(28) = 3.42, P = 0.002$, corrected $P = 0.010$, Cohen's $d = 0.64$), while a reverse pattern was found during retrieval ($t(24) = -2.61$, $P = 0.015$, corrected $P = 0.039$, Cohen's $d = 0.52$; 4 subjects were excluded from this analysis due to fewer than 10 trials in any condition, see Supplementary Table 4) (Fig. 4C). Lower pattern similarity for same-location pairs than near-distance pairs during retrieval was also found in CA1 ($t(24) = -2.81$, $P = 0.010$, corrected $P = 0.039$, Cohen's $d = 0.56$), but not in CA23DG ($t(24) = 0.37$, $P = 0.713$) (Fig. 4D), and there was a marginally significant region (CA1 vs. CA23DG) by location interaction ($F(1,24) = 4.07$, $P = 0.055$). Whole-brain searchlight analysis did not reveal any representation of location identity elsewhere in the brain.

To summarize, the above analyses revealed that the hippocampus subfields contained the representation of event structure: Whereas the CA1 contained information about the location identity, the CA23DG were sensitive to the sequential distance of the locations.

Hippocampal Sequence Boundary Effects during Encoding

In addition to spatial location and distance, the location structure also contains sequence boundaries. Unlike previous studies where the boundary was introduced by background context or different sequences (Ezzyat and Davachi 2014; Hsieh et al. 2014), the boundary in the current study was introduced by the repetition of the location sequence. That is, when the 11th word was presented, subjects would return to the first location, which would break the sequence contiguity. As a result, for a given temporal distance (e.g., 4), we can construct both within-boundary pairs (e.g., word 6 and word 10) and cross-boundary pairs (e.g., word 8 and word 12). Please note that the match of temporal distance would control the effect of autocorrelation of fMRI BOLD response. Since the items were randomly presented during retrieval, the temporal sequence was broken and no sequence boundary was still present; this analysis was only conducted for the encoding period.

To compare within versus cross-boundary pairs of matching distances, we analyzed temporal distances of 4–7 ordinal positions during encoding (Fig. 5A; Supplementary Table 5). Following a previous study (Ezzyat and Davachi 2014), we predicted that the similarity of neural representations would be higher for within-boundary pairs than cross-boundary pairs. Supporting this hypothesis, this effect was found in both CA1 ($t(28) = 3.70$, $P < 0.001$, corrected $P = 0.002$, Cohen's $d = 0.69$) and CA23DG ($t(28) = 4.37$, $P < 0.001$, corrected $P < 0.001$, Cohen's $d = 0.81$) (Fig. 5B). This effect was specific to the hippocampus and did not occur in EC or PHC, or in any other brain region in the whole-brain analysis.

Hippocampal Temporal Context Reinstatement during Retrieval

The above analyses reveal that hippocampal representational patterns are modified according to the well-trained structured location sequence, exhibiting representational transformation of spatial and sequential information, as well as sequence boundary effect to aid temporal order memory. In the following analysis, we further examined whether representations in hippocampal subfields also support another type of temporal order, that is, the episodic-like temporal context formed through one-shot learning. Due to the autocorrelation of the fMRI BOLD signal, we could not directly compare the representational similarity of temporally adjacent pairs with more distant pairs. Instead, previous studies have shown that the episodic-like temporal context formed during encoding could be reinstated during retrieval (Manning et al. 2011). We thus could examine the effects of temporal context during retrieval. In particular, for a given temporal distance (interval between 2 trials) during retrieval (TDr, ranging from 1 to 29 trials), we grouped the pairs, according to their temporal distance during encoding (TDe), into short ($TDe \leq 3$ trials) and long ($4 \leq TDe \leq 6$ trials) conditions (Fig. 6A). This grouping was motivated by the small number of trials of each individual distance and by previous findings that effects of temporal contexts decayed quickly beyond 3 items (Manning et al. 2011). We restricted the analysis to correct trials and $TDr \leq 20$ trials, as there were very few pairs for $TDr > 20$ trials (Supplementary Table 6). Each participant's pattern similarity was first averaged according to the 2 TDe conditions in each TDr and then was averaged across all the TDrs. We predicted that the brain regions containing representations of temporal context should show higher pattern similarity for short-distance pairs than long-distance pairs. Consistent with this prediction, we found this pattern in CA1 ($t(23) = 3.17$, $P = 0.004$, corrected $P = 0.021$, Cohen's $d = 0.65$; 4 subjects were excluded due to fewer than 10 trials in any condition, and one subject was excluded as an outlier, that is, 2.5 SDs above the mean, see Supplementary Table 7) (Fig. 6B). No temporal context reinstatement was found in any other brain region.

Control Analysis: The Hippocampal Representations Were Not Affected by the Landmark Type or Word Semantics

We did 2 control analyses to make sure our results were not confounded by the landmark type or the semantics of words in the study list. First, since 5 objects and 5 scenes were used as landmarks, the pattern similarity could be affected by different pair types (object–object, scene–scene, or object–scene). However, no significant effects of pair types were found in any of the above analyses in any hippocampal subregions (Supplementary Tables 8–12), and the statistics were very similar whether or not to control the pair types.

Second, in all the above analyses, we only considered the representation of the event structure and the temporal context, but not the representations of the word that were linked into each location, as previous studies did not reveal strong item representations in the hippocampus. To make sure the pattern similarity of hippocampal subfields represented the event structure and temporal context, rather than the semantic information, we conducted a latent semantic analysis to generate the semantic similarity matrix of the words, using a well-trained Chinese word embedding model, Directional Skip-Gram (Song et al. 2018). Correlating the semantic similarity with the neural representational similarity (Supplementary Method and Supplementary Fig. 10A) did not reveal significant semantic representation in any hippocampal subfield ($Ps > 0.05$) (Supplementary Fig. 10B). In addition, all the above results

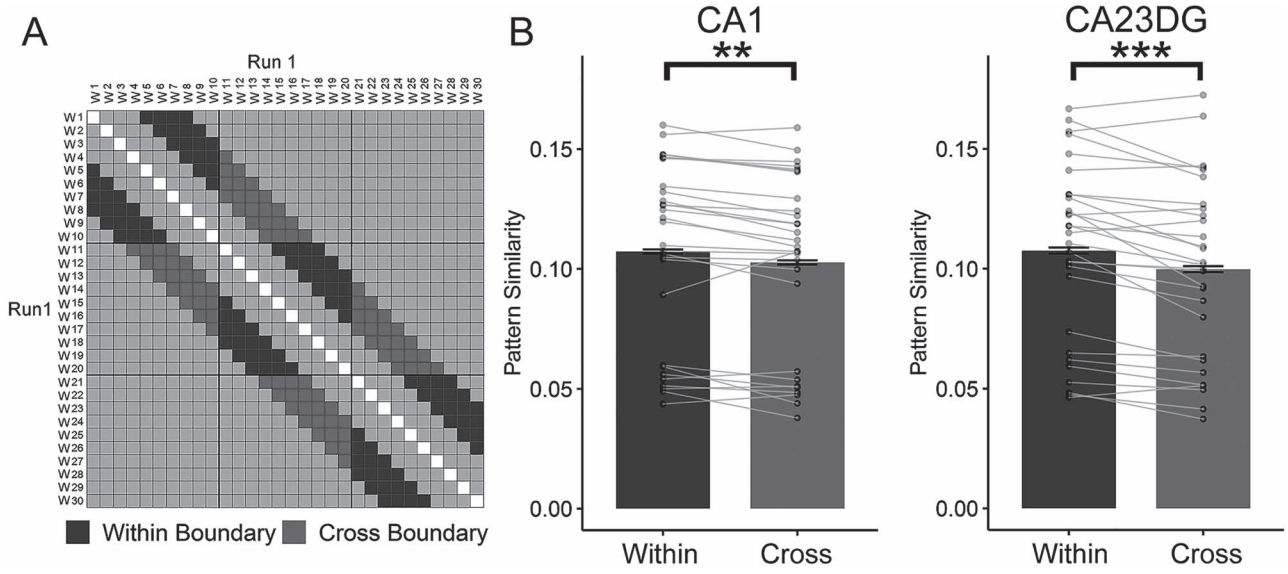

Figure 5. Sequence boundary representation during encoding. (*A*) Schematic depiction of within-boundary and cross-boundary word pairs. The black lines show the boundaries of the location sequence. (*B*) Pattern similarity for within-boundary and cross-boundary pairs in CA1 and CA23DG, showing higher pattern similarity for within-boundary pairs than cross-boundary pairs. Each line represents one subject and the bars represent the group means. Error bars indicate averaged within-subject standard errors. $^{**}P < 0.01$. $^{***}P < 0.001$.

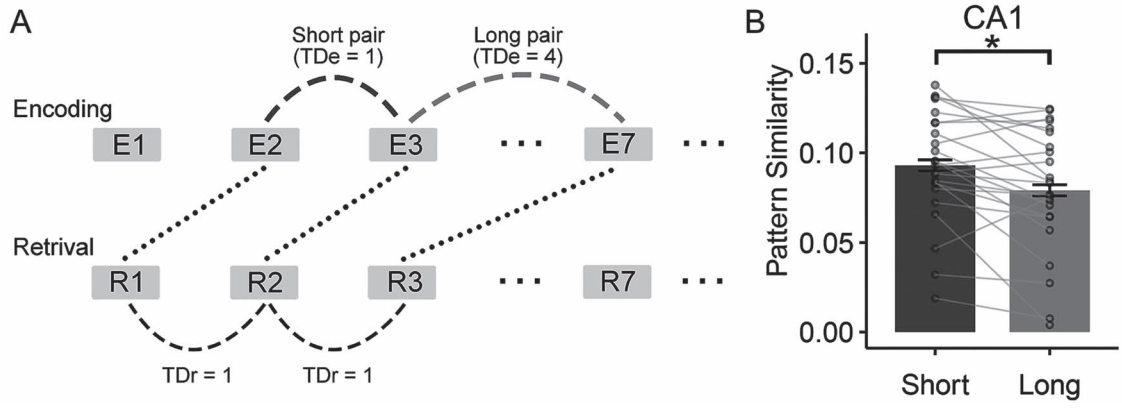

Figure 6. Temporal context reinstatement during retrieval. (*A*) Schematic depiction of temporal distance during encoding. For all pairs of trials with a given temporal distance during retrieval, they could be grouped, based on their temporal distance during encoding, into short-distance (TDe ≤ 3) or long-distance (4 ≤ TDe ≤ 6) pairs. The pattern similarity for each temporal distance during retrieval was first averaged and then averaged across all temporal distances. (*B*) Pattern similarity for short and long TDe pairs during retrieval. The CA1 area showed greater pattern similarity for short-distance pairs than long-distance pairs. Each line represents one subject and the bars represent the group means. Error bars indicate averaged within-subject standard errors. $^{*}P < 0.05$.

remained unchanged after controlling the semantic similarity. Interestingly, we found significant semantic representations during encoding in the ventromedial prefrontal cortex (vmPFC; $r(28) = 0.017$, $P = 0.032$) and a marginally significant effect in the SPL ($r(28) = 0.020$, $P = 0.063$).

Discussion

Inspired by the ancient mnemonics of MOL, the current study revealed a novel neural mechanism that supports precise temporal order memory of random events. The specific behavior patterns (e.g., primacy and recency effect according to the location sequence, and the high ratio of within-location swap errors to overall errors) indicated that subjects were correctly using the method of loci after extensive practices. The neural data indicate that, in addition to the hippocampal temporal context binding, the hippocampus also contained event structure representations during temporal order memory. These representations were shaped by 2 types of representational transformation processes acting on spatial locations and sequential sequences, which were associated with CA1 and CA23DG, respectively. These results emphasize the multiplexed and flexible nature of hippocampal representations in the service of precise temporal order memory.

Hippocampal Representation of Well-Trained Event Structure

Mounting evidence suggests that the hippocampal–entorhinal system can explicitly represent spatial sequences. First, the hippocampal–entorhinal system contains place cells (O'Keefe and Dostrovsky 1971) and grid cells (Hafting et al. 2005) that

provide 2 complementary representational metrics of spatial locations and distances, respectively. Second, the hippocampus exhibits specific neural mechanisms such as cross-frequency coupling of high-frequency bursts of activity to the phase of low-frequency oscillations, which may support the representation and pairwise binding of event sequences (Jensen and Lisman 2005; Axmacher et al. 2010; Heusser et al. 2016). Third, rodent studies analyzed activity while animals traveled along with well-trained spatiotemporal sequences and found that CA1 "time cells" showed context-specific activities at unique time points of an experience (MacDonald et al. 2011; MacDonald et al. 2013). A recent study revealed both types of temporal order representations, that is, encoding both temporal flow and trial structure, by the same alEC neurons (Tsao et al. 2018). Interestingly, in well-trained structured experiences, the encoding of temporal flow across trials was reduced, whereas the encoding of the trial structure was increased. Human neuroimaging studies have also found that both hippocampus (Deuker et al. 2016) and alEC (Bellmund et al. 2019) can represent well-studied event sequences or event maps. The hippocampus exhibits increased activity during events that violate an expected sequence (Kumaran and Maguire 2006; Chen et al. 2015) and shows increased within-sequence similarity and decreased between-sequence similarity (Kalm et al. 2013), as well as greater pattern similarity between adjacent items in well-learned object sequences than random sequences (Hsieh et al. 2014). Finally, the hippocampal representation is sensitive to sequence boundaries (Ezzyat and Davachi 2014; Hsieh et al. 2014).

Our results significantly extend these observations. First, the current study revealed all 3 types of event sequence representations in one single study, including spatial location representations, sequential distance representations, and sequence boundary representations. Together with the representation of temporal context, our study revealed the rich multiplexing of spatial, temporal, and sequential representations in the human hippocampus. This might not be possible without using the effective method of loci strategy.

Second, unlike previous studies, the loci map was not presented while subjects were encoding and retrieving the word list, suggesting that these event structure representations could be reinstated via conscious memory retrieval, resembling the spontaneous sequence replay during awake resting state and sleep in rodents (Skaggs and McNaughton 1996; Karlsson and Frank 2009) and humans (Kurth-Nelson et al. 2016; Liu et al. 2019). Third, while representations of sequential distance were restricted to CA23DG, we found significant temporal boundary effects in both CA1 and CA23DG. This is consistent with the proposal that both CA1 and CA3 are involved when memories for events must be held over long intervals (Farovik et al. 2010). Finally, several recent studies have implicated the alEC in temporal order memory (Tsao et al. 2018; Bellmund et al. 2019; Montchal et al. 2019), by representing the sequential event structure. The current study mainly found sequence representations in CA23DG. One obvious characteristic of the current study is that the sequential event structure was used as a scaffold for temporal order memory of words, with an emphasis on the binding of items into a structured context. Consistently, both human imaging and rodent studies have also implicated the hippocampus in context coding (Yonelinas et al. 2019). Future studies should further examine the role of alEC and hippocampal subfields in event structure representations and context binding.

Representational Transformations during the Use of the Method of Loci

Strikingly, we found clear evidence of representational transformations for both spatial and sequential information during the use of the method of loci. Transformation of spatial representations was found in CA1 during retrieval, revealing a pattern that is different from that in PHC during encoding. In the current study, each location was associated with 3 words, and consequently, there were significant within-location swap errors. To achieve high accuracy, the representations thus needed to be reconfigured in order to enable the encoding of multiple items into the same location and yet keep them separate. This requirement is similar to that during path disambiguation in both rodents and humans. For example, hippocampal representations of overlapping routes (Chanales et al. 2017) or object sequences (Hsieh et al. 2014) become more distinct than nonoverlapping routes/sequences. A previous rodent study also revealed that hippocampal neurons encoded different episodes in a task of overlapping sequences of odors (Ginther et al. 2011).

In addition to spatial representations, we observed significant representational transformations for sequences in CA23DG, a region that has been implicated in temporal pattern separation before (Madar et al. 2019). Unlikely the previous studies which found greater pattern similarity for temporally closer items in both alEC and hippocampus (Deuker et al. 2016; Bellmund et al. 2019), representations of more adjacent representations were more distinct in CA23DG. This pattern was different from the temporal context representation in CA1, which showed higher similarity for temporally adjacent than for more distant items. Together with the transformations of spatial representation, our results suggest that hippocampal representations can be flexibly configured in order to support temporal order memory. Interestingly, several cortical regions, including the right OP, bilateral LOC, left SMG/MTG, and left FP, showed greater pattern similarity to locations with a shorter distance, consistent with several previous studies (Jenkins and Ranganath 2010; Foudil et al. 2020). Future studies should further examine how the hippocampus and neocortical regions work together to support precise temporal order memory.

The flexible employment and reconfiguration of hippocampal spatial and temporal representations in support of episodic memory have been frequently reported in the literature. For example, one study found lower pattern similarity for spatially near items than spatially far items, but an opposite pattern for temporal representations (Kyle et al. 2015), whereas another study found greater pattern similarity for both spatially and temporally adjacent item pairs (Deuker et al. 2016). Still, the CA23DG showed lower pattern similarity when both spatial and temporal information was correctly retrieved (Copara et al. 2014). Another study reported that CA1 showed greater pattern similarity for trials that shared the same episodic context as compared to those with different episodic contexts, whereas CA23DG showed the opposite pattern (Dimsdale-Zucker et al. 2018). Clearly, future studies are required to examine in greater detail when hippocampal representations match temporal and spatial distances and when they disentangle these distances.

It should be noted that the isolation of spatial representations in the current study was achieved by comparing the same-location pairs with the near-distance pairs. As a result, we could not completely exclude the possibility that this contrast was also affected by the differences in sequential distance. Despite this caveat, we noticed that the CA1 was not sensitive to sequential

distance, suggesting the differences between the same-location and near-distance pairs in CA1 were mainly contributed by the location identity. Future studies could use a sequence with overlapping locations to disentangle the representation of spatial locations and sequential distances.

CA1 Temporal Context Reinstatement and Temporal Order Memory

The current study revealed clear evidence of temporal context reinstatement in the hippocampal CA1 area, with greater pattern similarity for item pairs studied at closer as compared to more distant temporal intervals. According to the temporal context or temporal drift model (Howard and Kahana 2002; Howard et al. 2005), an episodic element is "tagged" to the random and slowly changing neuronal background activity that is present at the time of encoding (Mankin et al. 2012). This temporal context is then reinstated during recall and provides information about the temporal distance by assessing the degree of disparity between the reinstated and the present neuronal background activity (Manning et al. 2011). Supporting the role of hippocampal temporal context in temporal order judgment, it has been shown that 1) lower hippocampal pattern similarity (i.e., higher representational distinctiveness) was associated with more accurate temporal order judgments (Jenkins and Ranganath 2016); 2) changes in EC pattern similarity during encoding of a narrative were correlated with later duration estimates between events (Lositsky et al. 2016); and 3) manipulation of context shifts by changing background images increased subjective feelings of temporal distance (Ezzyat and Davachi 2014). Our results add to this literature by showing hippocampal temporal context representations when subjects were asked to rely on existing sequence structure, suggesting that temporal context binding might be automatic.

Integration of Multiple Representational Formats Supports Temporal Order Memory

The current studies revealed rich spatial and temporal sequence coding in the hippocampus in a single memory task. A further question is how these representations are integrated to support highly precise episodic-like temporal order memory, which is usually not possible if not relying on the method of loci strategy. According to the cognitive map theory, the spatial representational formats of the hippocampal formation can support flexible cognition and behavior, including episodic memory (O'Keefe and Nadel 1978; Bellmund et al. 2018). Accordingly, it has been found that the same neurons represent information about both space and time (Kraus et al. 2013). This suggests that the 2 dimensions might be integrated into a common coding scheme of spatiotemporal proximity in the hippocampus, supporting the formation of hierarchical structures in a memory space (Eichenbaum et al. 1999; McKenzie et al. 2014; Collin et al. 2015). Human fMRI studies found that the spatial and temporal aspects of autobiographical experiences are coded within the hippocampus across various scales of magnitude, up to 1 month in time and 30 km in space (Nielson et al. 2015). After learning spatiotemporal trajectories in a large-scale virtual city, subject-specific neural similarity in the hippocampus scales with the remembered proximity of events in space and time (Deuker et al. 2016). The joint coding of space and temporal context found in CA1 in the current study further suggests that spatial information can be combined with temporal contexts in order to support temporal order memory.

Beyond the representation of space and time, our study further suggests that the learned structured event sequence may serve as a scaffold for the organization of temporal memory. In addition, a previous study showed that spatial and episodic information might be separately represented in different CA1 neurons, suggesting that in addition to place cells, other hippocampal neurons are involved in supporting episodic context coding (Tanaka et al. 2018). Finally, although the method of loci might not be commonly used, it represents just one particularly prominent case of learned and structured knowledge—that is, schemas—which have been consistently shown to be combined with learned material to facilitate episodic memory (Gilboa and Marlatte 2017; Xue 2018). This could be achieved via interactions between the hippocampus and vmPFC (van Kesteren et al. 2010; Preston and Eichenbaum 2013). Interestingly, we also found significant representations of learned words in the vmPFC during encoding. It is likely that via the interaction between vmPFC and hippocampus, the to-be-learnt words could be effectively linked to the well-learned structure, via semantic-based associations. All these rich representations might be integrated with the ongoing hippocampal oscillation to form an integrated sequence of neuronal activities that shapes our temporal order memory (Buzsáki and Llinás 2017). With proper behavioral and cognitive strategies, we could effectively engage these effective mechanisms to achieve striking memory outcomes. Future studies should uncover the intricate interaction of externally driven and internally organized sequences (that are influenced by long-term learning) in shaping our experiences and memories. For example, future studies could examine how the method of loci could modulate the effect of temporal distance on temporal order judgment (Kwok and Macaluso 2015). Furthermore, researchers could try to translate our paradigm into rodent or primate studies to uncover the neuronal mechanisms.

To summarize, using the method of loci to strongly engage the hippocampus, the current study uncovered rich and multiplexed spatial, temporal, and structured sequence representations in the hippocampus. Through transformations of spatial and sequential representations, the hippocampus generates robust and distinctive episodic contexts that are linked to the learned material. This provides a novel neural mechanism by which humans can achieve precise temporal order memory and also helps to uncover the mystery of this ancient mnemonic trick.

Supplementary Material

Supplementary material can be found at *Cerebral Cortex* online.

Funding

NSFC and the Israel Science Foundation (ISF) joint project (31861143040); National Science Foundation of China (31730038); 111 Project (B07008); Sino-German Collaborative Research Project "Crossmodal Learning" (NSFC 62061136001/DFG TRR169); Guangdong Pearl River Talents Plan Innovative and Entrepreneurial Team grant (#2016ZT06S220).

Notes

Conflict of Interest. The authors have no conflicts of interest to declare.

Authors' Contributions

Conceptualization: G.X.; Methodology: G.X., C.L., and Z.Y.; Software: C.L. and Z.Y.; Formal Analysis: G.X., C.L., and Z.Y.; Investigation: Z.Y.; Resources: G.X. and Z.Y.; Writing—Original Draft: G.X. and C.L.; Writing—Review & Editing: G.X., C.C., and N.A.; Visualization: C.L; Supervision: G.X.; Funding Acquisition: G.X.

References

Anderson JR. 1974. Retrieval of propositional information from long-term memory. *Cogn Psychol*. 6:451–474.

Avants BB, Epstein CL, Grossman M, Gee JC. 2008. Symmetric diffeomorphic image registration with cross-correlation: evaluating automated labeling of elderly and neurodegenerative brain. *Med Image Anal*. 12:26–41.

Axmacher N, Henseler MM, Jensen O, Weinreich I, Elger CE, Fell J. 2010. Cross-frequency coupling supports multi-item working memory in the human hippocampus. *Proc Natl Acad Sci*. 107:3228.

Bellmund JLS, Deuker L, Doeller CF. 2019. Mapping sequence structure in the human lateral entorhinal cortex. *elife*. 8:e45333.

Bellmund JLS, Gardenfors P, Moser EI, Doeller CF. 2018. Navigating cognition: spatial codes for human thinking. *Science*. 362:eaat6766.

Bender AR, Keresztes A, Bodammer NC, Shing YL, Werkle-Bergner M, Daugherty AM, Yu Q, Kühn S, Lindenberger U, Raz N. 2018. Optimization and validation of automated hippocampal subfield segmentation across the lifespan. *Hum Brain Mapp*. 39:916–931.

Buzsáki G, Llinás R. 2017. Space and time in the brain. *Science*. 358:482–485.

Chanales AJH, Oza A, Favila SE, Kuhl BA. 2017. Overlap among spatial memories triggers repulsion of hippocampal representations. *Curr Biol*. 27:2307–2317.e5.

Chen J, Cook PA, Wagner AD. 2015. Prediction strength modulates responses in human area CA1 to sequence violations. *J Neurophysiol*. 114:1227–1238.

Collin SHP, Milivojevic B, Doeller CF. 2015. Memory hierarchies map onto the hippocampal long axis in humans. *Nat Neurosci*. 18:1562–1564.

Cong S, Risacher SL, West JD, Wu Y-C, Apostolova LG, Tallman E, Rizkalla M, Salama P, Saykin AJ, Shen L. 2018. Volumetric comparison of hippocampal subfields extracted from 4-minute accelerated vs. 8-minute high-resolution T2-weighted 3T MRI scans. *Brain Imaging Behav*. 12:1583–1595.

Copara MS, Hassan AS, Kyle CT, Libby LA, Ranganath C, Ekstrom AD. 2014. Complementary roles of human hippocampal subregions during retrieval of spatiotemporal context. *J Neurosci*. 34:6834.

Cousineau D, O'Brien F. 2014. Error bars in within-subject designs: a comment on Baguley (2012). *Behav Res Methods*. 46:1149–1151.

Cox RW. 1996. AFNI: software for analysis and visualization of functional magnetic resonance Neuroimages. *Comput Biomed Res*. 29:162–173.

Dale AM, Fischl B, Sereno MI. 1999. Cortical surface-based analysis: I. segmentation and surface reconstruction. *NeuroImage*. 9:179–194.

Davachi L, DuBrow S. 2015. How the hippocampus preserves order: the role of prediction and context. *Trends Cogn Sci*. 19:92–99.

Deuker L, Bellmund JL, Navarro Schröder T, Doeller CF. 2016. An event map of memory space in the hippocampus. *elife*. 5:e16534.

Dimsdale-Zucker HR, Ritchey M, Ekstrom AD, Yonelinas AP, Ranganath C. 2018. CA1 and CA3 differentially support spontaneous retrieval of episodic contexts within human hippocampal subfields. *Nat Commun*. 9:294.

Dresler M, Shirer WR, Konrad BN, Müller NCJ, Wagner IC, Fernández G, Czisch M, Greicius MD. 2017. Mnemonic training reshapes brain networks to support superior memory. *Neuron*. 93:1227–1235.e1226.

Eichenbaum H. 2014. Time cells in the hippocampus: a new dimension for mapping memories. *Nat Rev Neurosci*. 15:732–744.

Eichenbaum H, Dudchenko P, Wood E, Shapiro M, Tanila H. 1999. The hippocampus, memory, and place cells: is it spatial memory or a memory space? *Neuron*. 23:209–226.

Esteban O, Markiewicz CJ, Blair RW, Moodie CA, Isik AI, Erramuzpe A, Kent JD, Goncalves M, DuPre E, Snyder M, et al. 2019. fMRIPrep: a robust preprocessing pipeline for functional MRI. *Nat Methods*. 16:111–116.

Ezzyat Y, Davachi L. 2014. Similarity breeds proximity: pattern similarity within and across contexts is related to later mnemonic judgments of temporal proximity. *Neuron*. 81:1179–1189.

Farovik A, Dupont LM, Eichenbaum H. 2010. Distinct roles for dorsal CA3 and CA1 in memory for sequential nonspatial events. *Learn Mem*. 17:12–17.

Favila SE, Chanales AJH, Kuhl BA. 2016. Experience-dependent hippocampal pattern differentiation prevents interference during subsequent learning. *Nat Commun*. 7:11066.

Fellner M-C, Volberg G, Wimber M, Goldhacker M, Greenlee MW, Hanslmayr S. 2016. Spatial mnemonic encoding: theta power decreases and medial temporal lobe BOLD increases co-occur during the usage of the method of loci. *Eneuro*. 3:ENEURO.0184–ENEU16.2016.

Foudil S-A, Kwok SC, Macaluso E. 2020. Context-dependent coding of temporal distance between cinematic events in the human precuneus. *J Neurosci*. 40:2129.

Gilboa A, Marlatte H. 2017. Neurobiology of schemas and schema-mediated memory. *Trends Cogn Sci*. 21:618–631.

Ginther MR, Walsh DF, Ramus SJ. 2011. Hippocampal neurons encode different episodes in an overlapping sequence of odors task. *J Neurosci*. 31:2706.

Gorgolewski KJ, Auer T, Calhoun VD, Craddock RC, Das S, Duff EP, Flandin G, Ghosh SS, Glatard T, Halchenko YO, et al. 2016. The brain imaging data structure, a format for organizing and describing outputs of neuroimaging experiments. *Sci Data*. 3:160044.

Greve DN, Fischl B. 2009. Accurate and robust brain image alignment using boundary-based registration. *NeuroImage*. 48:63–72.

Hafting T, Fyhn M, Molden S, Moser M-B, Moser EI. 2005. Microstructure of a spatial map in the entorhinal cortex. *Nature*. 436:801–806.

Heusser AC, Poeppel D, Ezzyat Y, Davachi L. 2016. Episodic sequence memory is supported by a theta–gamma phase code. *Nat Neurosci*. 19:1374–1380.

Hindy NC, Ng FY, Turk-Browne NB. 2016. Linking pattern completion in the hippocampus to predictive coding in visual cortex. *Nat Neurosci*. 19:665–667.

Howard MW, Fotedar MS, Datey AV, Hasselmo ME. 2005. The temporal context model in spatial navigation and relational

learning: toward a common explanation of medial temporal lobe function across domains. *Psychol Rev*. 112:75–116.
Howard MW, Kahana MJ. 2002. A distributed representation of temporal context. *J Math Psychol*. 46:269–299.
Hsieh LT, Gruber MJ, Jenkins LJ, Ranganath C. 2014. Hippocampal activity patterns carry information about objects in temporal context. *Neuron*. 81:1165–1178.
Jenkins LJ, Ranganath C. 2010. Prefrontal and medial temporal lobe activity at encoding predicts temporal context memory. *J Neurosci*. 30:15558–15565.
Jenkins LJ, Ranganath C. 2016. Distinct neural mechanisms for remembering when an event occurred. *Hippocampus*. 26:554–559.
Jenkinson M, Bannister P, Brady M, Smith S. 2002. Improved optimization for the robust and accurate linear registration and motion correction of brain images. *NeuroImage*. 17:825–841.
Jensen O, Lisman JE. 2005. Hippocampal sequence-encoding driven by a cortical multi-item working memory buffer. *Trends Neurosci*. 28:67–72.
Kalm K, Davis MH, Norris D. 2013. Individual sequence representations in the medial temporal lobe. *J Cogn Neurosci*. 25:1111–1121.
Karlsson MP, Frank LM. 2009. Awake replay of remote experiences in the hippocampus. *Nat Neurosci*. 12:913.
Kok P, Turk-Browne NB. 2018. Associative prediction of visual shape in the hippocampus. *J Neurosci*. 38:6888.
Kraus BJ, Robinson Ii RJ, White JA, Eichenbaum H, Hasselmo ME. 2013. Hippocampal "time cells": time versus path integration. *Neuron*. 78:1090–1101.
Kriegeskorte N, Goebel R, Bandettini P. 2006. Information-based functional brain mapping. *Proc Natl Acad Sci U S A*. 103:3863–3868.
Kriegeskorte N, Mur M, Bandettini P. 2008. Representational similarity analysis - connecting the branches of systems neuroscience. *Front Syst Neurosci*. 2:4.
Kumaran D, Maguire EA. 2006. An unexpected sequence of events: mismatch detection in the human hippocampus. *PLoS Biol*. 4:e424.
Kurth-Nelson Z, Economides M, Dolan RJ, Dayan P. 2016. Fast sequences of non-spatial state representations in humans. *Neuron*. 91:194–204.
Kwok SC, Macaluso E. 2015. Scale invariance of temporal order discrimination using complex, naturalistic events. *Cognition*. 140:111–121.
Kyle CT, Smuda DN, Hassan AS, Ekstrom AD. 2015. Roles of human hippocampal subfields in retrieval of spatial and temporal context. *Behav Brain Res*. 278:549–558.
Liu Y, Dolan RJ, Kurth-Nelson Z, Behrens TEJ. 2019. Human replay spontaneously reorganizes experience. *Cell*. 178:640–652. e614.
Lositsky O, Chen J, Toker D, Honey CJ, Shvartsman M, Poppenk JL, Hasson U, Norman KA. 2016. Neural pattern change during encoding of a narrative predicts retrospective duration estimates. *elife*. 5:e16070.
Maass A, Berron D, Libby LA, Ranganath C, Düzel E. 2015. Functional subregions of the human entorhinal cortex. *elife*. 4:e06426.
MacDonald CJ, Carrow S, Place R, Eichenbaum H. 2013. Distinct hippocampal time cell sequences represent odor memories in immobilized rats. *J Neurosci*. 33:14607.
MacDonald CJ, Lepage KQ, Eden UT, Eichenbaum H. 2011. Hippocampal "time cells" bridge the gap in memory for discontiguous events. *Neuron*. 71:737–749.
Madar AD, Ewell LA, Jones MV. 2019. Temporal pattern separation in hippocampal neurons through multiplexed neural codes. *PLoS Comput Biol*. 15:e1006932.
Maguire EA, Valentine ER, Wilding JM, Kapur N. 2003. Routes to remembering: the brains behind superior memory. *Nat Neurosci*. 6:90–95.
Mankin EA, Sparks FT, Slayyeh B, Sutherland RJ, Leutgeb S, Leutgeb JK. 2012. Neuronal code for extended time in the hippocampus. *Proc Natl Acad Sci*. 109:19462–19467.
Manning JR, Polyn SM, Baltuch GH, Litt B, Kahana MJ. 2011. Oscillatory patterns in temporal lobe reveal context reinstatement during memory search. *Proc Natl Acad Sci*. 108:12893–12897.
McKenzie S, Frank Andrea J, Kinsky Nathaniel R, Porter B, Rivière Pamela D, Eichenbaum H. 2014. Hippocampal representation of related and opposing memories develop within distinct, hierarchically organized neural schemas. *Neuron*. 83:202–215.
Montchal ME, Reagh ZM, Yassa MA. 2019. Precise temporal memories are supported by the lateral entorhinal cortex in humans. *Nat Neurosci*. 22:284–288.
Müller NCJ, Konrad BN, Kohn N, Muñoz-López M, Czisch M, Fernández G, Dresler M. 2018. Hippocampal-caudate nucleus interactions support exceptional memory performance. *Brain Struct Funct*. 223:1379–1389.
Mumford J. 2007. A guide to calculating percent change with Featquery. Unpublished Tech Report. Available from: http://mumford.bol.ucla.edu/perchange_guide.pdf.
Mumford JA, Turner BO, Ashby FG, Poldrack RA. 2012. Deconvolving BOLD activation in event-related designs for multivoxel pattern classification analyses. *NeuroImage*. 59:2636–2643.
Nielson DM, Smith TA, Sreekumar V, Dennis S, Sederberg PB. 2015. Human hippocampus represents space and time during retrieval of real-world memories. *Proc Natl Acad Sci*. 112:11078.
O'Keefe J, Dostrovsky J. 1971. The hippocampus as a spatial map: preliminary evidence from unit activity in the freely-moving rat. *Brain Res*. 34:171–175.
O'Keefe J, Nadel L. 1978. *The hippocampus as a cognitive map*. Oxford: Clarendon Press.
Preston AR, Eichenbaum H. 2013. Interplay of hippocampus and prefrontal cortex in memory. *Curr Biol*. 23:R764–R773.
Ranganath C, Hsieh LT. 2016. The hippocampus: a special place for time. *Ann N Y Acad Sci*. 1369:93–110.
Roediger HL. 1980. The effectiveness of four mnemonics in ordering recall. *J Exp Psychol Hum Learn Mem*. 6:558.
Skaggs WE, McNaughton BL. 1996. Replay of neuronal firing sequences in rat hippocampus during sleep following spatial experience. *Science*. 271:1870–1873.
Smith SM, Nichols TE. 2009. Threshold-free cluster enhancement: addressing problems of smoothing, threshold dependence and localisation in cluster inference. *NeuroImage*. 44:83–98.
Sone D, Sato N, Maikusa N, Ota M, Sumida K, Yokoyama K, Kimura Y, Imabayashi E, Watanabe Y, Watanabe M, et al. 2016. Automated subfield volumetric analysis of hippocampus in temporal lobe epilepsy using high-resolution T2-weighed MR imaging. *Neuroimage Clin*. 12:57–64.
Song Y, Shi S, Li J, Zhang H, editors. 2018. Directional Skip-Gram: explicitly distinguishing left and right context for word embeddings. In: *Proceedings of the 2018 Conference of the North American Chapter of the Association for Computational Linguistics: Human Language Technologies, Volume 2 (Short Papers)*. New Orleans (LA): Association for Computational Linguistics, pp. 175–180.

Tanaka KZ, He H, Tomar A, Niisato K, Huang AJY, McHugh TJ. 2018. The hippocampal engram maps experience but not place. *Science*. 361:392–397.

Thavabalasingam S, O'Neil EB, Lee ACH. 2018. Multivoxel pattern similarity suggests the integration of temporal duration in hippocampal event sequence representations. *NeuroImage*. 178:136–146.

Tsao A, Sugar J, Lu L, Wang C, Knierim JJ, Moser MB, Moser EI. 2018. Integrating time from experience in the lateral entorhinal cortex. *Nature*. 561:57–62.

Tulving E. 1985. How many memory systems are there? *Am Psychol*. 40:385.

Tustison NJ, Avants BB, Cook PA, Zheng Y, Egan A, Yushkevich PA, Gee JC. 2010. N4ITK: improved N3 bias correction. *IEEE Trans Med Imaging*. 29:1310–1320.

van Kesteren MTR, Fernández G, Norris DG, Hermans EJ. 2010. Persistent schema-dependent hippocampal-neocortical connectivity during memory encoding and postencoding rest in humans. *Proc Natl Acad Sci*. 107: 7550–7555.

Wagner IC, Konrad BN, Schuster P, Weisig S, Repantis D, Ohla K, Kühn S, Fernández G, Steiger A, Lamm C, et al. 2021. Durable memories and efficient neural coding through mnemonic training using the method of loci. *Sci Adv*. 7:eabc7606.

Xiao X, Dong Q, Gao J, Men W, Poldrack RA, Xue G. 2017. Transformed neural pattern reinstatement during episodic memory retrieval. *J Neurosci*. 37:2986.

Xue G. 2018. The neural representations underlying human episodic memory. *Trends Cogn Sci*. 22:544–561.

Yonelinas AP, Ranganath C, Ekstrom AD, Wiltgen BJ. 2019. A contextual binding theory of episodic memory: systems consolidation reconsidered. *Nat Rev Neurosci*. 20:364–375.

Yushkevich PA, Pluta JB, Wang H, Xie L, Ding S-L, Gertje EC, Mancuso L, Kliot D, Das SR, Wolk DA. 2015. Automated volumetry and regional thickness analysis of hippocampal subfields and medial temporal cortical structures in mild cognitive impairment. *Hum Brain Mapp*. 36:258–287.

Zeidman P, Maguire EA. 2016. Anterior hippocampus: the anatomy of perception, imagination and episodic memory. *Nat Rev Neurosci*. 17:173–182.